Amino Acids (2013) 44:1205–1214
DOI 10.1007/s00726-012-1454-0

ORIGINAL ARTICLE

A quantitative analysis of spontaneous isoaspartate formation from N-terminal asparaginyl and aspartyl residues

Bert H.-O. Güttler · Holger Cynis · Franziska Seifert · Hans-Henning Ludwig · Andrea Porzel · Stephan Schilling

Received: 18 September 2012 / Accepted: 24 December 2012 / Published online: 24 January 2013

Abstract The formation of isoaspartate (isoAsp) from asparaginyl or aspartyl residues is a spontaneous post-translational modification of peptides and proteins. Due to isopeptide bond formation, the structure and possibly function of peptides and proteins is altered. IsoAsp modifications within the peptide chain have been reported for many cytosolic proteins. Amyloid peptides (Aβ) deposited in Alzheimer's disease may carry an N-terminal isoAsp-modification. Here, we describe a quantitative investigation of isoAsp-formation from N-terminal Asn and Asp using model peptides similar to the Aβ N-terminus. The study is based on a newly developed separation of peptides using capillary electrophoresis (CE). ^{1}H NMR was employed to validate the basic finding of N-terminal isoAsp-formation from Asp and Asn. Thereby, the isomerization of Asn at neutral pH (0.6 day^{-1}, peptide NGEF) is approximately six times faster than that within the peptide chain (AANGEF). The difference in velocity between Asn and Asp isomerization is approximately 50-fold. In contrast to N-terminal Asn, Asp isomerization is significantly accelerated at acidic pH. The kinetic solvent isotope (k_{D2O}/k_{H2O}) effect of 2.46 suggests a rate-limiting proton transfer in isoAsp-formation. The proton inventory is consistent with transfer of one proton in the transition state, supporting the previous notion of rate-limiting deprotonation of the peptide backbone amide during succinimide-intermediate formation. The study provides evidence for a spontaneous N-terminal isoAsp-formation within peptides and might explain the accumulation of N-terminal isoAsp in amyloid deposits.

Keywords Alzheimer's disease · PIMT · Capillary electrophoresis · ^{1}H NMR · Isoaspartate

B. H.-O. Güttler · H. Cynis · F. Seifert · H.-H. Ludwig · S. Schilling (✉)
Probiodrug AG, Weinbergweg 22, Biozentrum, 06120 Halle (Saale), Germany
e-mail: stephan.schilling@probiodrug.de

Present Address:
H. Cynis
Brigham and Women's Hospital, Harvard Medical School, NRB 363, 77 Avenue Louis Pasteur, Boston, MA 02115, USA

Present Address:
F. Seifert
Institute of Pharmacy, Martin-Luther-University Halle-Wittenberg, Weinbergweg 22, 06120 Halle (Saale), Germany

A. Porzel
Department of Bioorganic Chemistry, Leibniz Institute of Plant Biochemistry, Weinberg 3, 06120 Halle (Saale), Germany

Introduction

The formation of isoaspartate (isoAsp) from asparagine (L-Asn) or aspartate (L-Asp) represents one common post-translational modification, which is considered to determine the half-life of proteins (Robinson and Rudd 1974; Robinson and Robinson 2001; Robinson et al. 1970). Under mild chemical or physiological conditions, L-Asn and L-Asp peptide bonds form a succinimide under consecutive release of ammonia (Robinson et al. 1970; Fig. 1) or water, respectively. The intermediate is prone to spontaneous hydrolysis resulting in the formation of isoAsp or Asp. Usually, L-asparaginyl residues decompose into L-isoAsp and L-Asp in a ratio of approximately 3:1 to 5:1, depending on the buffer and pH conditions (Meinwald et al. 1986; Geiger and Clarke 1987; Patel and Borchardt 1990). Epimerization of the succinimide-intermediate may

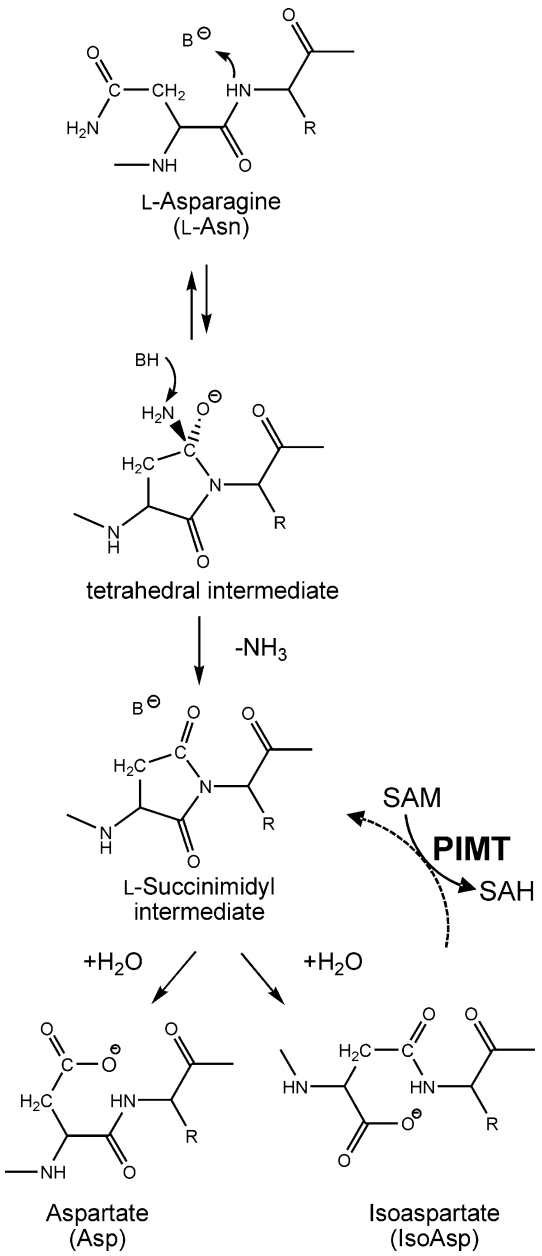

Fig. 1 Spontaneous deamidation of L-asparaginyl residues. Deamidation leads to formation of a succinimidyl intermediate that is hydrolyzed to aspartyl or isoaspartyl residues. The formation and resolution of the tetrahedral intermediate to form the succinimidyl intermediate involves proton transition(s). L-aspartyl residues are also undergoing such reactions (not shown) but at slower rate. On the state of the succinimidyl intermediate, epimerization at the Cα carbon might occur (not shown) leading to minute amounts of D-aspartyl and D-isoaspartyl residues. L-isoaspartyl and D-aspartyl residues are prone to methylation by PIMT, building up protein repair mechanism of the cells (Lowenson and Clarke 1992)

lead to generation of minute amounts of D-isoAsp and D-Asp.

The isoAsp-formation introduces an additional methylene group into the backbone of the protein or peptide (Aswad et al. 2000; Geiger and Clarke 1987), consequently altering its structure. Therefore, the isoAsp-modification may cause also different protein function (George-Nascimento et al. 1990; Velazquez et al. 1997; Noguchi 2010; Corti and Curnis 2011). It was suggested that Asn—because of a rapid isomerization as compared with Asp functions as a molecular timer for protein ageing, development, protein turnover and other biological events (Robinson et al. 1970; Robinson 1974; Robinson and Robinson 2001). The enzyme protein L-isoaspartyl *O*-methyltransferase (PIMT, EC 2.1.1.77) represents a cellular repair mechanism to recycle isoAsp- to Asp-residues (Clarke 1985). PIMT utilizes the cofactor *S*-adenosylmethionine (SAM) to transfer a methyl group onto the α-carboxyl group of isoAsp leading to succinimidyl intermediate formation followed by subsequent hydrolysis to L-Asp and L-isoAsp (compare to Fig. 1). Known substrates of PIMT comprise the histone proteins H2A and H2B or synapsin I and II (Young et al. 2001, 2005; Carter and Aswad 2008). Recent results suggest that PIMT might also act as marker for protein degradation as shown for p53 (Lee et al. 2012), initiator for chromatin remodeling as shown for histone H2A and H2B or function as transcription activator (Park et al. 2012).

Possibly caused by lower protein turnover during ageing and pathogenesis, the formation of isoAsp has been implicated in the pathogenesis of autoimmune and neurodegenerative disorders. A detailed characterization of Aβ-peptides and neurofibrillary tangles deposited in Alzheimer's disease revealed presence of isoAsp in substantial quantity (Saido et al. 1996; Shimizu et al. 2000). Isomerization of Asp^1 and Asp^7 within the Aβ sequence ($D^1AEFRHD^7SGYE…40/42$) has been reported, which has been shown to enhance its fibril formation propensity (Roher et al. 1993; Saido et al. 1996). Previous studies revealed that isoAsp influences also the susceptibility of the amyloid precursor protein to cleavage and thereby the molecular pathways of Aβ production: Formation of isoAsp at position 1 of Aβ enhanced cleavage by Cathepsin B, an alternative β-secretase, whereby cleavage by the β-secretase BACE 1 was not detected (Böhme et al. 2008a, b). Thus, occurrence of isoAsp within the peptide chain of APP might occur prior to Aβ release and, therefore, account for isoAsp-modified Aβ within deposits.

To further investigate the formation of isoAsp in peptides, we aimed at an analysis of N-terminal isoAsp-formation. Because previous studies did not focus on such analysis, we developed a new assay based on the separation of model peptides using capillary electrophoresis (CE-UV). The results should provide further insights into the role and formation of isoAsp at the N-terminus, which might have also implications for, e.g., stability of protein drugs.

Materials and methods

Synthesis and purification of model peptides

Peptides were generated as C-terminal amides in a 0.5 mmol scale on an automated peptide synthesizer (Endeavour 90, AAPPTec) using Fmoc strategy. The peptides were synthesized on a Rink Amide MBHA resin (MERCK Biosciences). A twofold excess of Fmoc-AA-OH and 2-(1H-benzotriazol-1-yl)-1,1,3,3-tetramethyluronium tetrafluoroborate (TBTU) in dimethylformamide (DMF) and 4 eq. *N*,*N*-Diisopropylethylamine for the coupling process were used. The reaction time was approximately 25 min and each coupling step was repeated for one time. For de-protection of the Fmoc group, a 20 % piperidine solution in DMF was applied. The peptides were cleaved from the resin with a mixture of 95 % trifluoroacetic acid (TFA), 2.5 % water and 2.5 % triisopropylsilane (TIS) for 2 h. The product was evaporated and re-crystallized from cold methanol/ether. The crude products were purified by RP-HPLC on a Luna 10 µm C18 column (100 Å, 250 × 21.20 mm, Phenomenex) applying an acetonitrile/water gradient (0.04 % TFA).

Analysis of isoAsp-formation using capillary electrophoresis (CE-UV)

Peptides were incubated at 37 °C using a sample buffer containing 12.5 mM sodium acetate, 12.5 mM 2-(*N*-Morpholino)ethanesulfonic acid (MES) and 25.0 mM Tris(hydroxymethyl)aminomethane (Tris) ensuring a constant ionic strength over a broad pH range (Ellis and Morrison 1982). In addition, 0.02 % (w/v) sodium azide was added to preserve sterile conditions. The pH value was adjusted by hydrochloric acid or sodium hydroxide. The incubation time ranged from minutes to months depending on the peptide and the pH value.

The peptides have been separated using a P/ACE™ MDQ Glycoprotein System (Beckman Coulter™, USA, Reorder No.: 338472) equipped with a capillary tubing of 30 cm in length, 50 µm inner diameter. The separation was accomplished in 50 mM citric acid, pH 2.0 at 20 °C. The absorption was detected at a wavelength of 200 ± 5 nm. The peptides NGEF, DGEF, D_{iso}GEF, NAEF, DAEF, D_{iso}AEF and $D_{(OMe)}$GEF have been separated at 20 kV and 0.2 psi. Acetyl-NGEF, Acetyl-DGEF and Acetyl-D_{iso}GEF have been separated at 20 kV without applying additional pressure. AANGEF, AADGEF and AAD_{iso}GEF have been analyzed at 5 kV without pressure. After every run, the capillary was flushed with 0.2 M NaOH, 1.0 N HCl followed by running buffer. The data were evaluated by comparing the peak areas of the model peptides and the internal standard peptide HY.

^{1}H nuclear magnetic resonance

^{1}H NMR spectra were recorded at 25 °C on an Agilent VNMRS 600-MHz spectrometer equipped with an inverse detection cryoprobe. NMR samples contained 1.73 mM of peptide in buffer without addition of D_2O. 40 transients were acquired. The water signal was suppressed using a 2 s pre-saturation pulse. A 90° excitation pulse (6.1 µs) was used with a pulse repetition rate of 15 s.

Determination of pK_a values

Titrations have been conducted using a Mettler Toledo DL50 Graphix equipped with a DG111-SC glass electrode. Standard solutions of 0.1 N NaOH and 0.1 N HCl (Roth, Karlsruhe, Germany) were applied. The peptides were dissolved in distilled water and pre-incubated at 37 °C. The titration was performed at 37 °C and the curve was evaluated using DL50 Graphix software. Each determination has been performed in triplicate at least.

Solvent isotope effect and proton inventory

To determine the kinetic solvent isotope effect (KIE) of the isomerization process, all buffers were prepared in water or deuterium oxide. The pH and pD values have been adjusted according to the formula: pD = (pH reading) + 0.4 (Cook 1991). The solvent KIE ($k_{(D2O)}/k_{(H2O)}$) of isoAsp-formation was determined with NGEF and $D_{(OMe)}$GEF in three-component buffer (12.5 mM MES, 12.5 mM acetic acid, 25 mM Tris) at pH/pD 8.0 and additionally for NGEF in tricine buffer at pH/pD 8.0 to rule out potential influence of buffer ions.

To assess the proton inventory, the sample buffer was prepared using H_2O and D_2O (at pH = pD) as solvent and mixed. Thereafter, 1 mM of the peptides (NGEF or $D_{(OMe)}$GEF) were dissolved in H_2O- and D_2O-containing sample buffer at pH/pD 8.0. Both peptide solutions were mixed in ratios of 80 % (v/v) H_2O to 20 % (v/v) D_2O; 60 % (v/v) H_2O to 40 % (v/v) D_2O; 40 % (v/v) H_2O to 60 % (v/v) D_2O and 20 % (v/v) H_2O to 80 % (v/v) D_2O. All peptide solutions were incubated at 37 °C and subsequently analyzed by CE-UV. For analysis, the isomerization velocity was plotted against the mole fraction of D_2O. The resulting graph was analyzed using the program "GraphPad Prism 4" from GraphPad Software Inc.

Results

Capillary electrophoresis for analysis of N-terminal isoAsp-formation

In a first attempt to chromatographically separate the model peptides NGEF, DGEF and D_{iso}GEF, HPLC using a

standard C-18 column was performed. A baseline separation could not be achieved (data not shown).

However, based on different p*K*a values of Asp and isoAsp with regard to the carboxylic group [i.e., Asp: $pK_{a,\ \alpha\text{-COOH}} = 1.99$, $pK_{a,\ \beta\text{-COOH}} = 3.90$ (Wagenknecht and Knapp 2009)], the formation of isoAsp was expected to result in a switch of the net charge of the peptides at acidic pH. As a consequence, the electrophoretic movement should change, with isoAsp-modified peptides migrating slower than the corresponding Asp and Asn containing peptides. Indeed, choosing an acidic pH of 2.0 as electrolyte solution, a separation of NGEF, DGEF and D_{iso}GEF was observed (Fig. 2a). In addition, an internal standard (the dipeptide HY) was baseline-separated from the standard peptides.

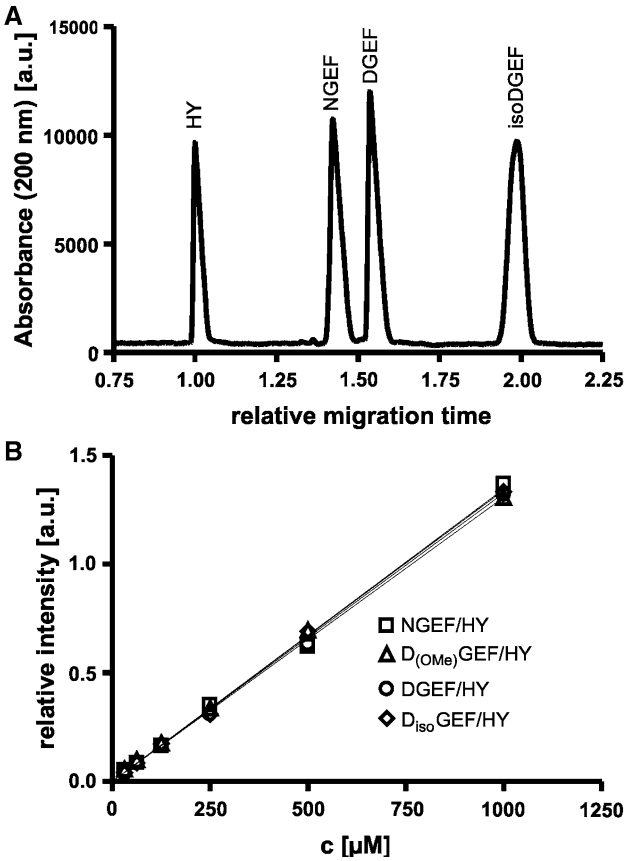

Fig. 2 **a** Separation of the peptides NGEF, DGEF and D_{iso}GEF and the standard peptide HY using capillary electrophoresis. The peptides were detected by UV absorption at 200 nm. To standardize the separation, the relative migration time is shown, applying HY as standard. Accordingly, HY is detected at a relative migration time of 1, followed by NGEF at 1.4, DGEF at 1.6 and D_{iso}GEF at 2. **b** Dependence of the relative absorption of NGEF, $D_{(OMe)}$GEF, DGEF and D_{iso}GEF on the peptide concentration after separation and detection. HY served as the internal standard peptide. The concentration of the model peptide has been plotted against the quotient of peak area of the model peptide divided by the peak area of the internal standard peptide. Virtually identical slopes suggest equivalent concentrations and absorption of the peptide standards, enabling analysis of deamidation/isoAsp-formation

To standardize separation conditions in different approaches, the relative migration time was calculated on the basis of the internal standard. Accordingly, HY possessed a relative migration time of 1 (actual migration time 2.6 min), followed by NGEF at 1.4 min, DGEF at 1.55 min and D_{iso}GEF at a migration time of 2.0 min (Fig. 2a). A similar separation was observed with the other model peptides in this study (see below, data not shown). In either case, the order of migration was as shown in Fig. 2a, suggesting that the differences in the p*K*a values caused by isoAsp-formation always result in changes of the net charge, making CE a valuable tool to analyze peptide conversion in a quantitative manner.

For evaluation of the isoAsp content, the internal standard peptide HY was applied at a constant concentration, and the relative UV signal areas at 200 nm calculated. A linear relationship of the ratio was observed within a broad concentration range (Fig. 2b).

Quantitative analysis of N-terminal isoAsp-formation

To investigate the N-terminal isoAsp-formation, a model peptide (NGEF), which was designed to show a rapid

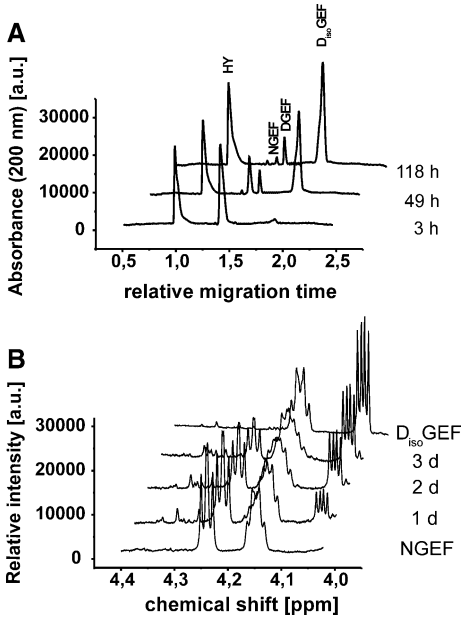

Fig. 3 **a** Spontaneous formation of D_{iso}GEF and DGEF from NGEF at 37 °C and pH 7.0. The model peptide NGEF (1 mM) was incubated for the indicated times, samples removed and the peptide composition analyzed using CE-UV. Upon incubation, the signal for NGEF decreases accompanied by increased signals of D_{iso}GEF. **b** Spontaneous deamidation of NGEF, assessed using ^{1}H NMR. The model peptide NGEF was incubated at pH 7.0 and 37 °C. Samples were removed after the indicated times and analyzed by ^{1}H NMR. The integral of the superimposed E H-α signals of both NGEF and D_{iso}GEF (approx. 4.16 ppm) was used as an internal standard. NGEF and D_{iso}GEF are characterized by the well-separated H-α signals of N (4.23 ppm) and D_{iso} (4.05 ppm), respectively

Table 1 Quantitative analysis of isoAsp-formation determined by CE-UV and ^{1}H NMR

Incubation time (h) of NGEF (1 mg/mL) at 37 °C and pH 7.0	^{1}H NMR [D_{iso}GEF] (%)	CE-UV [D_{iso}GEF] (%)
24	15	18
48	24	26
72	37	40

Illustrated is the comparison of generated amount of IsoAsp from 1 mg/mL NGEF after incubation for 24, 48 and 72 h at 37 °C and pH 7. The quantification was carried out by ^{1}H NMR and by CE-UV

deamidation due to the adjacent Gly residue, was incubated at 37 °C and pH 7. At different time points, samples were taken and the peptides separated using CE-UV. As shown in Fig. 3a, during the incubation period of 118 h a significant formation of D_{iso}GEF could be observed. Moreover, minute amounts were already detectable after 3 h of incubation. As expected, also DGEF originating from deamidation of NGEF occurred in the mixture leading to a final ratio of D_{iso}GEF:DGEF of approximately 9:1.

To validate these results, in a following approach the formation of isoAsp at the N-terminus was assessed using ^{1}H NMR (Fig. 3b). Proton spectra of the model peptides NGEF, DGEF and D_{iso}GEF were recorded for signal assignment. For quantification, the integral intensities of the well-separated H-α signals of N and D_{iso} were used, normalized to the integral of the superimposed E H-α signals of both, NGEF and D_{iso}GEF. The ^{1}H NMR-based quantification shows good conformity with the results of the capillary electrophoresis analysis (Table 1). On the basis of this validation, the further analysis of spontaneous isoAsp-formation in DGEF, NAEF, DAEF, $_{(Ac)}$NGEF, AANGEF and $D_{(OMe)}$GEF was evaluated using CE-UV.

Rate of spontaneous isoAsp-formation in different model peptides

In a first approach to quantify the spontaneous deamidation of NGEF, we investigated the progress of D_{iso}GEF and DGEF formation at pH 9.0 (Fig. 4a). The rapid decomposition of NGEF was accompanied by formation of D_{iso}GEF. Also DGEF was formed, however, the concentration was always below 10 %, indicating that N-terminal deamidation to form Asp is virtually negligible. The decomposition rate fits best to a first-order kinetic model, as suggested by linearization of the data (Fig. 4b).

To evaluate the rate of spontaneous isoAsp-formation, several model peptides with Asx at the N-terminus or within the peptide chain have been investigated at different pH conditions. The rate of spontaneous isoAsp-formation from N-terminal Asn in NGEF was clearly pH-dependent

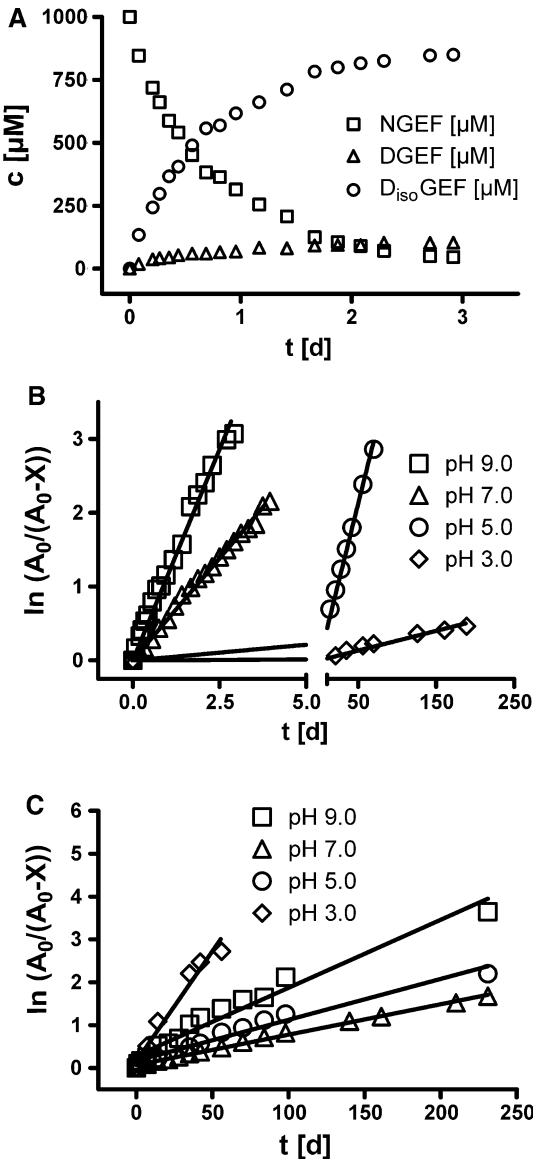

Fig. 4 Analysis of spontaneous deamidation/isoAsp-formation from NGEF and DGEF. **a** Formation of D_{iso}GEF and DGEF from NGEF at pH 9.0 and 37 °C; **b** Decomposition of NGEF at pH 3, 5, 7 and 9; **c** Formation of D_{iso}GEF from DGEF at pH 3, 5, 7 and 9. The peptides were incubated at 37 °C and samples were removed consecutively. The concentration of the peptides has been determined using CE-UV as described before. Data have been analyzed according to a model of first order, as indicated by the linearization. A_0 refers to the initial concentration of the Asx peptide, X denotes the concentration of product at a given time

(Fig. 4b). The rate of spontaneous deamidation and isoAsp formation was fastest at basic pH and strictly declined at acidic pH. The deamidation of Asn thereby yields Asp and isoAsp residues at a pH-independent ratio of ~1:9, efficiently ruling out deamidation leading directly to Asp, which accords to previous observations (Capasso et al. 1993). Also N-terminal Asp was found to isomerize over time (Fig. 4c), although at significantly lower rate. In

contrast to deamidation of Asn, the rate of isomerization was low at neutral pH. The highest rate of isoAsp-formation was observed at acidic pH.

The kinetic data of spontaneous deamidation and Asp isomerization of all peptides investigated are summarized in Table 2. In general, the isoAsp-formation from Asn was found to be fastest at basic pH, whereas N-terminal Asp-residues show fastest spontaneous isomerization under basic and acidic conditions and a corresponding minimum between pH 5 and 7. At neutral pH-conditions, deamidation of Asn in NGEF is about 60 times faster than isoAsp-formation from DGEF. The difference was significantly lower with NAEF and DAEF, suggesting a differential influence of the second amino acid on velocity of isoAsp-formation. At pH 3.0, isoAsp is even faster generated from N-terminal Asp as compared with N-terminal Asn.

To investigate the role of the free α-amino group for spontaneous isoAsp-formation, we assessed acetylated NGEF [$_{(Ac)}$NGEF]. As depicted in Table 2, the pH-dependency of the isomerization of $_{(Ac)}$NGEF was similar to NGEF, however, the rate of isomerization was eightfold slower. This was further substantiated by analysis of the peptide AANGEF, which showed a similar rate of isoAsp-formation as compared with $_{(Ac)}$NGEF (Table 2). The results point to an accelerated isomerization of peptides carrying a free α-amino group without effect on the relative pH-dependence of the reaction.

To illustrate the role of the β-carboxyl group for D_{iso}GEF formation from DGEF, the isomerization velocity of an activated form of DGEF ($D_{(OMe)}$GEF) was determined. Methylation of the side chain led to significant increase of the reaction velocity by factors of 14 and 740 as compared with NGEF and DGEF, respectively (Table 2). The acceleration factor was 3,000-fold as compared with DGEF at pH 9.0.

Solvent isotope effect on isoAsp-formation

To analyze, whether proton transfer is rate limiting for N-terminal isoAsp-formation, we incubated peptides in deuterium oxide (Fig. 5a). The isomerization of NGEF and $D_{(OMe)}$GEF at pH/pD 8.0 was significantly lower in D_2O. The quantitative analysis of the isomerization velocities revealed a KIE of 2.46 for NGEF and 2.42 for $D_{(OMe)}$GEF, suggesting that the transfer of at least one proton is rate-limiting in the isomerization reaction.

In a separate investigation, we assessed the dependence of the velocity on pD (Table 3). The rate dependence mirrored that observed in H_2O, suggesting slower isoAsp-formation at low pD. The relative drop in the rate was stronger in D_2O, resulting in an increasing solvent isotope effect with decreasing pH/pD.

Table 2 Decomposition velocities of various model peptides

pH value	NGEF [k (day^{-1})]	DGEF [k (day^{-1})]	NAEF [k (day^{-1})]	DAEF [k (day^{-1})]	$D_{(OMe)}$GEF [k (day^{-1})]	$_{(Ac)}$NGEF [k (day^{-1})]	AANGEF [k (day^{-1})]	AADGEF [k (day^{-1})]
9	1.21 ± 0.04	0.028 ± 0.003	0.045 ± 0.001	0.0145 ± 0.0004	83 ± 2	0.49 ± 0.02	0.48 ± 0.01	0.0173 ± 0.0005
8	0.94 ± 0.02	0.025 ± 0.003	0.0411 ± 0.0004	0.0127 ± 0.0002	13.1 ± 0.2	0.27± 0.02	0.29 ± 0.01	n.d.
7	0.57 ± 0.01	0.0097 ± 0.0004	0.029 ± 0.001	0.0088 ± 0.0004	7.1 ± 0.1	0.075± 0.003	0.087 ± 0.005	0.015 ± 0.001
6	0.23 ± 0.01	0.0092 ± 0.0001	0.0177 ± 0.0003	0.00111 ± 0.00004	4.4 ± 0.1	0.019 ± 0.001	0.031 ± 0.001	n.d.
5	0.044 ± 0.001	0.016 ± 0.001	0.0060 ± 0.0002	0.00156 ± 0.00002	1.28 ± 0.04	0.003 ± 0.001	0.0064 ± 0.0004	n.d.
4	0.0099 ± 0.0003	0.042 ± 0.001	0.0036 ± 0.0001	0.0034 ± 0.0001	0.33 ± 0.01	0.0017 ± 0.0001	0.0023 ± 0.0001	0.012 ± 0.001
3	0.0025 ± 0.0001	0.083 ± 0.005	0.0022 ± 0.0001	0.0097 ± 0.0004	0.082 ± 0.002	0.00074 ± 0.00004	0.00102 ± 0.00005	0.017± 0.002

Mapped are the decomposition velocities of NGEF, DGEF, NAEF, DAEF, $D_{(OMe)}$GEF, $_{(Ac)}$NGEF, AANGEF and AADGEF at 37 °C from pH 3 to pH 9

n.d. not determined

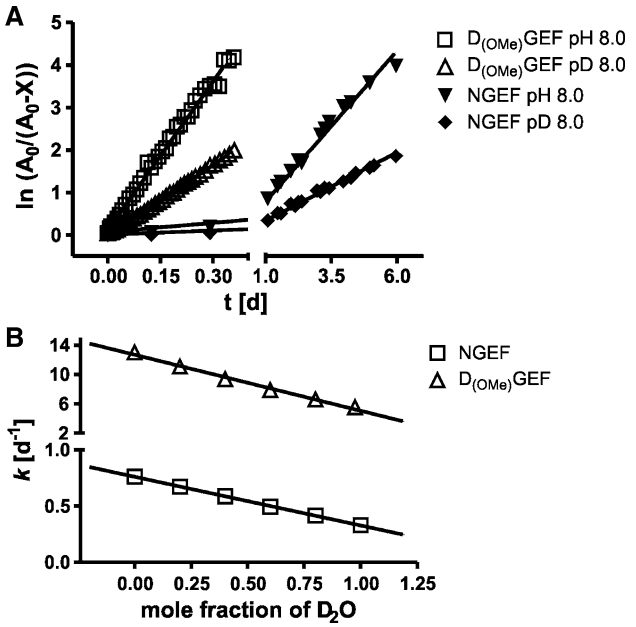

Fig. 5 **a** Spontaneous deamidation of NGEF and formation of D_{iso}GEF from $D_{(OMe)}$GEF in deuterium oxide (D_2O). Both peptides (1 mM) have been incubated at 37 °C and pH/pD 8. The data were analyzed as before and the kinetic isotope effect (KIE) calculated from k_{H2O} and k_{D2O}. The resulting KIE was 2.46 for NGEF and 2.42 for $D_{(OMe)}$GEF. **b** Dependence of the rate constant of D_{iso}GEF formation on the mole fraction of deuterium in the sample (proton inventory). NGEF (*squares*) and $D_{(OMe)}$GEF (*triangles*, 1 mM both) were incubated in mixtures of buffers (pH/pD 8.0), which have been prepared with H_2O or D_2O. The resulting rate constants were plotted depending on the mole fraction of deuterium in solution. The data are consistent with transfer of one proton in the transition state. A_0 refers to the initial concentration of the Asx peptide, X denotes the concentration of product at a given time

To further study the reaction, we determined the rate constants in mixtures of H_2O and D_2O and plotted the rate against the mole fractions of D_2O (Fig. 5b). The proton inventory is consistent with transfer of a single proton in the transition state.

Discussion

The N-terminus of peptides and proteins might be prone to different post-translational modifications such as acylation or formation of pyroglutamic acid from glutaminyl and glutamyl precursors. In contrast to these modifications, which are catalyzed by different transferases, the N-terminal formation of isoAsp is considered a purely spontaneous reaction in vitro and in vivo. Here, we investigated the rate and mechanism of N-terminal isomerization of Asn- and Asp-residues, which may constitute the N-Terminus of amyloid peptides deposited in Alzheimer's disease.

Previous studies to analyze the isoAsp-formation within the peptide chain were based on separation of products using HPLC (Stephenson and Clarke 1989; Patel and Borchardt 1990; Capasso et al. 1993). Novel approaches also relied on degradation of peptides using endoprotease Asp-N and electron transfer dissociation (ETD) mass spectrometry (Sargaeva et al. 2011; Ni et al. 2010). Because the previous HPLC methods are not capable of separating peptides with an N-terminal isoAsp from the precursors, we here employed CE-UV for analysis. The method takes advantage of the different p*K*a values of the carboxyl groups in Asp and isoAsp at acidic pH. Because the basic principle of different net charge of Asn, Asp and isoAsp at pH of 2–3 applies generally, we used CE-UV also for assessment of isoAsp-formation within the peptide chain enabling a comparison. Under the applied conditions, capillary electrophoresis allowed the analysis of the sample within less than 8 min, requiring a sample volume of 5 µl. Thus, the newly introduced method provides an opportunity to rapidly analyze Asx isomerization, which might have also implications for other experimental approaches such as analysis of isoAsp-peptide conversion by protein isoaspartyl methyltransferase (PIMT).

Table 3 Kinetic isotope Effect in dependence of pH/pD value for $D_{(OMe)}$GEF

pD/pH	$D_{(OMe)}$GEF [k_{D2O} (day^{-1})]	KIE [k_{H2O}/k_{D2O}]
8	5.42 ± 0.04	2.42
7	2.79 ± 0.03	2.56
5	0.38 ± 0.01	3.36
3	0.0218 ± 0.0004	3.75

Displayed is the decomposition velocity of $D_{(OMe)}$GEF at pD 3, 5, 7 and 8 and the resulting kinetic isotope effect (KIE) at each pD value. The KIE is increasing with decreasing pH/pD value

The formation of isoAsp at the N-terminus proceeds readily at neutral pH. The calculated half-lives range from 79 days for the Aβ-sequence DAEF to 140 min for the isomerization of $D_{(OMe)}$GEF. Although we observed an accelerated peptide bond degradation with NGEF compared to the modified N-termini in $_{(Ac)}$NGEF and AAN-GEF, the half–lives determined are within the range of those reported previously for different proteins and peptides (Stephenson & Clarke 1989; Geiger & Clarke 1987), which are 1-100 days for Asn and 40-300 days for Asp, depending on the peptide sequence. In accordance with our analysis, the Asx-Gly linkages are rapidly degrading peptide bonds. Thus, the general requirements and mechanism of the reactions appear to follow the same principle. Such a conclusion is finally also supported by our initial mechanistic analysis. The data clearly suggest a differential pH-dependence of isomerization between Asn and Asp residues. In contrast, modification of Asp in $D_{(OMe)}$GEF results in a similar pH-rate profile as observed with Asn (Table 2).

Thus, the rate of isomerization is generally determined by the electrophilicity of the β-carbonyl carbon. Likewise, because the side chain of Asp is protonated at pH < 3.0, the rate of nucleophilic attack by the nitrogen of the Asx-AA linkage and the Asp β-carbonyl carbon increases. The significant enhancement of isoAsp-formation from $D_{(OMe)}$GEF and the pH-dependence are all consistent with a rate-determining formation of the succinimidyl-intermediate (which is identical formed from NGEF, DGEF and $D_{(OMe)}$GEF). It has been suggested previously that a deprotonation of the attacking nitrogen might be determining for the rate of the overall reaction at pH < 3 (Capasso et al. 1993) (see also Fig. 1). The solvent kinetic isotope effect and the proton inventories of our study clearly support such a conclusion. The equal size of the isotope effect and the slope of unity obtained with NGEF and $D_{(OMe)}$GEF support transfer of one single proton in the transition state. The general finding of a rate-limiting proton transfer is, however, not surprising because numerous acyl transfer reactions have been described for which such limiting factors are concluded (Satterthwait and Jencks 1974; Cox and Jencks 1978; Barnett and Jencks 1969).

It remains unclear, though, whether a formation of isoAsp at the N-terminus affects the function of certain proteins in a similar manner as described for isoAsp within the peptide chain (George-Nascimento et al. 1990; Velazquez et al. 1997; Weber and McFadden 1997; Corti and Curnis 2011). Considering the half-lives of N-terminal Asx of days to months to form isoAsp, the turnover of most intracellular proteins is probably too high (Varshavsky 1996) to yield accumulation of the N-terminally modified proteins in considerable amounts. In contrast, amyloid peptides deposited in extracellular space such as Aβ have been described to contain isoAsp at the N-terminus and within the chain, possibly due to low if any turnover (Roher et al. 1993; Lowenson et al. 1994; Saido et al. 1996). These observations are also in line with the enzymatic properties and distribution of PIMT. Previous studies on the substrate specificity of PIMT suggested that conversion of isoAsp strongly depends on the size and amino acid constitution of the substrate (Lowenson and Clarke 1990; Lowenson and Clarke 1991). Already these studies pointed towards an exceptionally inefficient conversion of a dipeptide containing isoAsp at the N-terminus (Lowenson and Clarke 1991). Likewise, in initial experiments we observed only poor methylation of isoDAEF by PIMT (not shown). Moreover, previous studies revealed that PIMT is primarily distributed to intracellular compartments or may be retained within the endoplasmatic reticulum (MacLaren et al. 1992; Potter et al. 1992; Lowenson et al. 1994). Thus, extracellular Aβ might escape the cellular isoAsp repair system (Lowenson et al. 1994).

In addition to isoAsp formation, also other post-translational modifications of amyloid peptides have been described (He and Barrow 1999; Schilling et al. 2006; Kummer et al. 2011). Among those, N-terminally truncated and pyroglutamate (pE) modified Aβ (Aβ3pE-42) gained considerable interest due to high aggregation propensity and oligomer toxicity (Schlenzig et al. 2009; Nussbaum et al. 2012). Compared with spontaneous formation of pE at the N-terminus of Aβ, which exhibits a half-life of ~10 years at neutral pH (Seifert et al. 2009), the N-terminal isoAsp-formation in the model peptide DAEF (representing the N-terminus of Aβ 1–4) is rather fast (78 days). In contrast to isoAsp, however, pE-formation has been shown to be matter of enzymatic catalysis in vivo (Schilling et al. 2004, 2008). Hence, the results of the present study can be reconciled with a spontaneous formation of N-terminal isoAsp after generation and deposition of Aβ in AD pathology. However, it should be considered that previous studies have shown that isoAsp-modifications in the Aβ precursor protein APP alter the processing and the liberation of Aβ (Böhme et al. 2008b). These reports are accompanied by several epidemiological studies that point to a crucial influence of the sequence surrounding the β-secretase cleavage site for generation of the N-terminus of Aβ (Haass et al. 1995; Di Fede et al. 2009; Jonsson et al. 2012). Therefore, it cannot be excluded that an isoAsp-formation—at least partially—precedes the APP cleavage, which, in turn, modifies the cellular processing.

In summary, we performed the first quantitative analysis of isoAsp-formation at the N-terminus of model peptides. The study has been enabled by introducing CE-UV for separation and quantification of substrates and products. Compared to in-chain Asx residues, the half-lives of the N-terminal sites appear shorter; however, the rate constants are generally within the range of those described previously. The results provide some clues for the appearance of isoAsp at the N-terminus of deposited amyloid peptides, and might be also important for other proteins which are stored for prolonged time, e.g., protein drugs.

Acknowledgments We are grateful to Prof. Dr. H.-U. Demuth for his helpful comments and suggestions on the manuscript. We thank Dr. T. Hoffmann for his technical support. This work was financially supported by the Investitionsbank Sachsen-Anhalt, Grant# 1004/00082 to Probiodrug AG (StS).

Conflict of interest BG, HC, FS, H-HL and StS are former or present employees of Probiodrug AG.

References

Aswad DW, Paranandi MV, Schurter BT (2000) Isoaspartate in peptides and proteins: formation, significance, and analysis. J Pharm Biomed Anal 21:1129–1136

Barnett RE, Jencks WP (1969) Diffusion-controlled proton transfer in intramolecular thiol ester aminolysis and thiazoline hydrolysis. J Am Chem Soc 91:2358–2369

Böhme L, Bär JW, Hoffmann T, Manhart S, Ludwig HH, Rosche F, Demuth HU (2008a) Isoaspartate residues dramatically influence substrate recognition and turnover by proteases. Biol Chem 389:1043–1053

Böhme L, Hoffmann T, Manhart S, Wolf R, Demuth HU (2008b) Isoaspartate containing amyloid precursor protein derived peptides alter efficacy and specificity of potential beta-secretases. Biol. Chem. 389:1055–1066

Capasso S, Mazzarella L, Sica F, Zagari A, Salvadori S (1993) Kinetics and mechanism of succinimide ring formation in the deamidation process of asparagine residues. J Chem Soc Perkin Trans 2:679–682

Carter WG, Aswad DW (2008) Formation, localization, and repair of L-isoaspartyl sites in histones H2A and H2B in nucleosomes from rat liver and chicken erythrocytes. Biochemistry 47: 10757–10764

Clarke S (1985) Protein carboxyl methyltransferases: two distinct classes of enzymes. Annu Rev Biochem 54:479–506

Cook PF (1991) Enzyme mechanism from isotope effects. CRC press, Boca Raton

Corti A, Curnis F (2011) Isoaspartate-dependent molecular switches for integrin-ligand recognition. J Cell Sci 124:515–522

Cox MM, Jencks WP (1978) General acid catalysis of the aminolysis of phenyl acetate by a preassociation mechanism. J Am Chem Soc 100:5956–5957

Di Fede G, Catania M, Morbin M, Rossi G, Suardi S, Mazzoleni G, Merlin M, Giovagnoli AR, Prioni S, Erbetta A, Falcone C, Gobbi M, Colombo L, Bastone A, Beeg M, Manzoni C, Francescucci B, Spagnoli A, Cantù L, Del Favero E, Levy E, Salmona M, Tagliavini F (2009) A recessive mutation in the APP gene with dominant-negative effect on amyloidogenesis. Science 323: 1473–1477

Ellis KJ, Morrison JF (1982) Buffers of constant ionic strength for studying pH-dependent processes. Methods Enzymol 87:405–426

Geiger T, Clarke S (1987) Deamidation, isomerization, and racemization at asparaginyl and aspartyl residues in peptides. Succinimide-linked reactions that contribute to protein degradation. J Biol Chem 262:785–794

George-Nascimento C, Lowenson J, Borissenko M, Calderon M, Medina-Selby A, Kuo J, Clarke S, Randolph A (1990) Replacement of a labile aspartyl residue increases the stability of human epidermal growth factor. Biochemistry 29:9584–9591

Haass C, Lemere CA, Capell A, Citron M, Seubert P, Schenk D, Lannfelt L, Selkoe DJ (1995) The Swedish mutation causes early-onset Alzheimer's disease by beta-secretase cleavage within the secretory pathway. Nat Med 1:1291–1296

He W, Barrow CJ (1999) The A beta 3-pyroglutamyl and 11-pyroglutamyl peptides found in senile plaque have greater beta-sheet forming and aggregation propensities in vitro than full-length A beta. Biochemistry 38:10871–10877

Jonsson T, Atwal JK, Steinberg S, Snaedal J, Jonsson PV, Bjornsson S, Stefansson H, Sulem P, Gudbjartsson D, Maloney J, Hoyte K, Gustafson A, Liu Y, Lu Y, Bhangale T, Graham RR, Huttenlocher J, Bjornsdottir G, Andreassen OA, Jonsson EG, Palotie A, Behrens TW, Magnusson OT, Kong A, Thorsteinsdottir U, Watts RJ, Stefansson K (2012) A mutation in APP protects against Alzheimer's disease and age-related cognitive decline. Nature 488:96–99

Kummer MP, Hermes M, Delekarte A, Hammerschmidt T, Kumar S, Terwel D, Walter J, Pape HC, König S, Roeber S, Jessen F, Klockgether T, Korte M, Heneka MT (2011) Nitration of tyrosine 10 critically enhances amyloid β aggregation and plaque formation. Neuron 71:833–844

Lee JC, Kang SU, Jeon Y, Park JW, You JS, Ha SW, Bae N, Lubec G, Kwon SH, Lee JS, Cho EJ, Han JW (2012) Protein L-isoaspartyl methyltransferase regulates p53 activity. Nat. Commun. 3:927

Lowenson JD, Clarke S (1990) Identification of isoaspartyl-containing sequences in peptides and proteins that are usually poor substrates for the class II protein carboxyl methyltransferase. J Biol Chem 265:3106–3110

Lowenson JD, Clarke S (1991) Structural elements affecting the recognition of L-isoaspartyl residues by the L-isoaspartyl/D-aspartyl protein methyltransferase. Implications for the repair hypothesis. J Biol Chem 266:19396–19406

Lowenson JD, Clarke S (1992) Recognition of D-aspartyl residues in polypeptides by the erythrocyte L-isoaspartyl/D-aspartyl protein methyltransferase. Implications for the repair hypothesis. J Biol Chem 267:5985–5995

Lowenson JD, Roher AE, Clarke S (1994) Protein aging extracellular amyloid formation and intracellular repair. Trends Cardiovasc Med 4:3–8

MacLaren DC, Kagan RM, Clarke S (1992) Alternative splicing of the human isoaspartyl protein carboxyl methyltransferase RNA leads to the generation of a C-terminal -RDEL sequence in isozyme II. Biochem Biophys Res Commun 185:277–283

Meinwald YC, Stimson ER, Scheraga HA (1986) Deamidation of the asparaginyl-glycyl sequence. Int J Pept Protein Res 28:79–84

Ni W, Dai S, Karger BL, Zhou ZS (2010) Analysis of isoaspartic acid by selective proteolysis with Asp-N and electron transfer dissociation mass spectrometry. Anal Chem 82:7485–7491

Noguchi S (2010) Conformational variation revealed by the crystal structure of RNase U2A complexed with Ca ion and 2′-adenylic acid at 1.03 Å resolution. Protein Pept Lett 17:1559–1561

Nussbaum JM, Schilling S, Cynis H, Silva A, Swanson E, Wangsanut T, Tayler K, Wiltgen B, Hatami A, Ronicke R, Reymann K, Hutter-Paier B, Alexandru A, Jagla W, Graubner S, Glabe CG, Demuth HU, Bloom GS (2012) Prion-like behaviour and tau-dependent cytotoxicity of pyroglutamylated amyloid-beta. Nature 485:651–655

Park JW, Lee JC, Ha SW, Bang SY, Park EK, Yi SA, Lee MG, Kim DS, Nam KH, Yoo JH, Kwon SH, Han JW (2012) Requirement of protein l-isoaspartyl *O*-methyltransferase for transcriptional activation of trefoil factor 1 (TFF1) gene by estrogen receptor alpha. Biochem Biophys Res Commun 420:223–229

Patel K, Borchardt RT (1990) Chemical pathways of peptide degradation. II. Kinetics of deamidation of an asparaginyl residue in a model hexapeptide. Pharm Res 7:703–711

Potter SM, Johnson BA, Henschen A, Aswad DW, Guzzetta AW (1992) The type II isoform of bovine brain protein L-isoaspartyl methyltransferase has an endoplasmic reticulum retention signal (…RDEL) at its C-terminus. Biochemistry 31:6339–6347

Robinson AB (1974) Evolution and the distribution of glutaminyl and asparaginyl residues in proteins. Proc Natl Acad Sci USA 71:885–888

Robinson NE, Robinson AB (2001) Molecular clocks. Proc Natl Acad Sci USA 98:944–949

Robinson AB, Rudd CJ (1974) Deamidation of glutaminyl and asparaginyl residues in peptides and proteins. Curr Top Cell Regul 8:247–295

Robinson AB, McKerrow JH, Cary P (1970) Controlled deamidation of peptides and proteins: an experimental hazard and a possible biological timer. Proc Natl Acad Sci USA 66:753–757

Roher AE, Lowenson JD, Clarke S, Wolkow C, Wang R, Cotter RJ, Reardon IM, Zurcher-Neely HA, Heinrikson RL, Ball MJ (1993) Structural alterations in the peptide backbone of beta-amyloid core protein may account for its deposition and stability in Alzheimer's disease. J Biol Chem 268:3072–3083

Saido TC, Yamao-Harigaya W, Iwatsubo T, Kawashima S (1996) Amino- and carboxyl-terminal heterogeneity of beta-amyloid peptides deposited in human brain. Neurosci Lett 215:173–176

Sargaeva NP, Lin C, O'Connor PB (2011) Differentiating N-terminal aspartic and isoaspartic acid residues in peptides. Anal Chem 83:6675–6682

Satterthwait AC, Jencks WP (1974) The mechanism of the aminolysis of acetate esters. J Am Chem Soc 96:7018–7031

Schilling S, Hoffmann T, Manhart S, Hoffmann M, Demuth HU (2004) Glutaminyl cyclases unfold glutamyl cyclase activity under mild acid conditions. FEBS Lett 563:191–196

Schilling S, Lauber T, Schaupp M, Manhart S, Scheel E, Bohm G, Demuth HU (2006) On the seeding and oligomerization of pGlu-amyloid peptides (in vitro). Biochemistry 45:12393–12399

Schilling S, Zeitschel U, Hoffmann T, Heiser U, Francke M, Kehlen A, Holzer M, Hutter-Paier B, Prokesch M, Windisch M, Jagla W, Schlenzig D, Lindner C, Rudolph T, Reuter G, Cynis H, Montag D, Demuth HU, Rossner S (2008) Glutaminyl cyclase inhibition attenuates pyroglutamate Abeta and Alzheimer's disease-like pathology. Nat Med 14:1106–1111

Schlenzig D, Manhart S, Cinar Y, Kleinschmidt M, Hause G, Willbold D, Funke SA, Schilling S, Demuth HU (2009) Pyroglutamate formation influences solubility and amyloidogenicity of amyloid peptides. Biochemistry 48:7072–7078

Seifert F, Schulz K, Koch B, Manhart S, Demuth HU, Schilling S (2009) Glutaminyl cyclases display significant catalytic proficiency for glutamyl substrates. Biochemistry 48:11831–11833

Shimizu T, Watanabe A, Ogawara M, Mori H, Shirasawa T (2000) Isoaspartate formation and neurodegeneration in Alzheimer's disease. Arch Biochem Biophys 381:225–234

Stephenson RC, Clarke S (1989) Succinimide formation from aspartyl and asparaginyl peptides as a model for the spontaneous degradation of proteins. J Biol Chem 264:6164–6170

Varshavsky A (1996) The N-end rule: functions, mysteries, uses. Proc Natl Acad Sci USA 93:12142–12149

Velazquez P, Cribbs DH, Poulos TL, Tenner AJ (1997) Aspartate residue 7 in amyloid beta-protein is critical for classical complement pathway activation: implications for Alzheimer's disease pathogenesis. Nat Med 3:77–79

Wagenknecht H-A, Knapp H (2009) Roempp Online. Version 3.5

Weber DJ, McFadden PN (1997) Injury-induced enzymatic methylation of aging collagen in the extracellular matrix of blood vessels. J Protein Chem 16:269–281

Young AL, Carter WG, Doyle HA, Mamula MJ, Aswad DW (2001) Structural integrity of histone H2B in vivo requires the activity of protein L-isoaspartate *O*-methyltransferase, a putative protein repair enzyme. J Biol Chem 276:37161–37165

Young GW, Hoofring SA, Mamula MJ, Doyle HA, Bunick GJ, Hu Y, Aswad DW (2005) Protein L-isoaspartyl methyltransferase catalyzes in vivo racemization of aspartate-25 in mammalian histone H2B. J Biol Chem 280:26094–26098